Multimodal Non-Rigid Registration Methods Based on Demons Models and Local Uncertainty Quantification Used in 3D Brain Images

Isnardo Reducindo[1,⋆], Aldo R. Mejía-Rodríguez[1], Edgar Arce-Santana[1,⋆⋆], Daniel U. Campos-Delgado[1], Elisa Scalco[2], Giovanni M. Cattaneo[3], and Giovanna Rizzo[2]

[1] Facultad de Ciencias, Universidad Autónoma de San Luis Potosí, S.L.P., México
[2] Institute of Molecular Bioimaging and Physiology (IBFM)-CNR, Milan, Italy
[3] Medical Physics Department, Ospedale San Raffaele, Scientific Institute, Milan, Italy
isnardo@fc.uaslp.mx

Abstract. In this work, we propose a novel fully automated method to solve the 3D multimodal non-rigid image registration problem. The proposed strategy overcomes the monomodal intensity restriction of fluid-like registration (FLR) models, such as Demons-based registration algorithms, by applying a mapping that relies on an intensity uncertainty quantification in a local neighbourhood, bringing the target and source images into a common domain where they are comparable, no matter their image modalities or mismatched intensities between them. The proposed methodology was tested with T1, T2 and PD weighted brain magnetic resonance (MR) images with synthetic deformations, and CT-MR brain images from a radiotherapy clinical case. The performance of the proposed approach was evaluated quantitatively by standard indices that assess the correct alignment of anatomical structures of interest. The results obtained in this work show that the addition of the local uncertainty mapping properly resolve the monomodal restriction of FLR algorithms when same anatomic counterparts exists in the images to register, and suggest that the proposed strategy can be an option to achieve multimodal 3D registrations.

1 Introduction

Image registration (IR) is the process of determining the spatial correspondence between objects in two or more images by finding a geometrical transformation that aligns a source image with a target one [1]. This process could be divided into two main streams: rigid registration (RR), and non-rigid registration (NRR) methods [2]. Rigid registration is a well-posed problem [1, 2], which is based on a global transformation that preserve the distance between all points in the image, and is described by a small set of parameters (shifts, scales and rotations).

⋆ I. Reducindo was supported by CONACYT doctoral scholarship No. 218513.
⋆⋆ This work was supported by CONACYT through grants No. 168140.

G. Bebis et al. (Eds.): ISVC 2014, Part II, LNCS 8888, pp. 11–20, 2014.

On the other hand, NRR is a more complex and involved problem, because the geometrical transformation may differ for each voxel in the image [3]. In medical imaging, IR is an important task due to its variety of clinical applications [4], such as the integration of multimodal information acquired with different scanners and at different times, or the optimization of an adaptive radiotherapy planning by assessing organ deformation induced by the radiotherapy treatment [5], among others. In this context, RR is mainly used to correct small misalignments in medical imaging. Meanwhile, NRR methods are used under complex deformations such as anatomical motions or morphological changes.

Due the relevance of the NRR applications, a great number of approaches to solve this problem have been reported in the literature [1–5], which could be classified depending on the alignment philosophy: based on geometrical features, or pixel/voxel property-based methods. In the first category, corresponding landmarks or surfaces are used to find the existing deformation between the studied images [6]. These techniques have the advantage of being more locally accurate, but the accuracy of these IR methods strictly depends on the user's ability to set corresponding landmarks/surfaces in the images to be registered; where this ad hoc procedure is a challenging task in multimodal or noisy images. On the other hand, pixel/voxel property-based methods use only voxels information to optimize a similarity metric [7] (mutual information, cross correlation, etc.), in order to recover the spatial transformation usually adopting a free-form structure as the deformation model [8]. Fluid-like registration (FLR) algorithms, such as optical flow (OF) and Demons-based [9, 10], are also well-known techniques belonging to the category of pixel/voxel property-based approaches, where the key idea is to consider that the intensity differences between the analyzed images can be described by the motion of voxels among them, making possible to find a displacement field by matching the intensity gradients between both images. In a clinical context, FLR methods, in particular Demons-based algorithms, are extensively used due to its ability of providing both good accuracy and performance [11], being more efficient in terms of computation time with respect to the free-form models. Nonetheless, an important restriction of these approaches is the hypothesis of intensity consistency between the analyzed images, restricting the algorithm to monomodal cases or images with matched intensities. Under this context, this work pursues to overcome the intensity dependence of Demons-based approaches by applying a mapping based on the intensity uncertainty of neighborhood voxels, which transforms the registering images to a common domain where the images can be compared.

The paper is organized as follows: in section 2, the theoretical bases and methods used in this work are presented; in subsection 2.1, the local intensity mapping is detailed, and in subsection 2.2 the proposed multimodal NRR algorithm is established. In section 3, the experiments performed to evaluate the algorithm are described and the obtained results are discussed. Finally, in section 4 the main conclusions of this work are outlined and the future work to improve the proposed methodology is established.

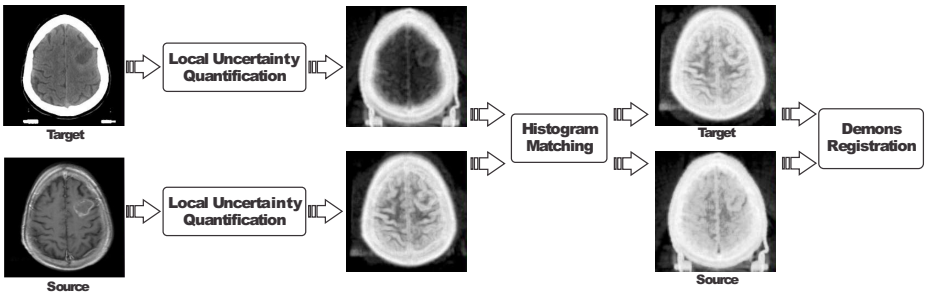

Fig. 1. Flowchart of the proposed multimodal non-rigid registration algorithm based on LUQ mapping

2 Methodology

The NRR can be formulated as an optimization problem that aims to find the spatial transformation model $\Phi : \mathbb{R}^3 \mapsto \mathbb{R}^3$ over each voxel of a source image $I_S(\cdot)$, so that it is aligned with a target one $I_T(\cdot)$. We can represent the spatial transformations as a displacements vector field $d(\cdot)$, which is added to the identity to get the non-parametric transformation $\Phi(\mathbf{r}) = \mathbf{r} + d(\mathbf{r})$, where $\mathbf{r} = (x, y, z)^\top$ denotes a position within the volume lattice $\Omega \subset \mathbb{R}^3$. Under this assumption and considering that the intensities between the registered images have homogeneous variations, the NRR can be formulated from the fallowing observation model

$$I_T(\mathbf{r}) = (I_S \circ \Phi)\mathbf{r} + \eta(\mathbf{r}), \tag{1}$$

where $\eta(\mathbf{r})$ represents random samples of independent and identically distributed (*i.i.d.*) Gaussian noise, with zero mean and variance $\sigma_\eta^2 > 0$. A similarity metric $\mathrm{SM}(\cdot,\cdot)$ is next considered between both images according to the observation model in eq. (1), for example the mean-squared error which forms the basis of intensity-based registration:

$$\mathrm{SM}(I_T, I_S \circ \Phi) = \frac{1}{2} \sum_{\mathbf{r}\in\Omega} \left\| I_T(\mathbf{r}) - I_S\left(\mathbf{r} + d(\mathbf{r})\right) \right\|^2, \tag{2}$$

where $\|\cdot\|$ denotes the Euclidean norm. A simple optimization process of eq. (2) over the space of non-parametric transformations Φ leads to an ill-posed problem with unstable and non-smooth solutions. To avoid this problem, and possibly to add some a priori knowledge, a regularization term $\mathrm{Reg}(\cdot)$ is often added to the similarity metric in eq. (2) in order to obtain a well-posed global energy function with a scaling by the variance of the noise term $\frac{1}{\sigma_\eta^2}$:

$$\Psi(d) = \frac{1}{\sigma_\eta^2}\mathrm{SM}(I_T, I_S \circ \Phi) + \frac{1}{\lambda}\mathrm{Reg}(d), \tag{3}$$

where $\lambda > 0$ denotes the regularization weight in the approximation problem. Thus, the cost function in eq. (3) is the basis of FLR methods.

According to eq. (3), the NRR problem can be formulated as the estimation of the OF between the images (I_T, I_S) [9]. The OF is a well-posed problem and many techniques have been proposed in the literature to estimate it [12]. For comparison purposes during the evaluation section, the method employed in this work to estimate the OF is based on a linearization of the SM in eq. (2) by conducting a first order Taylor approximation, and a regularization term with the structure of a quadratic potential based on a probabilistic approach in the form of a prior random Markov field [13]. On the other hand, Thirion developed a very efficient solution scheme for the optimization of eq. (3), based on adapting Maxwell's demons to a diffusion-based method [14]. The idea of Demons-based NRR considers I_S as a deformable grid, which is diffused through the contours of the objects in I_T by the action of effectors, called Demons. Both OF and Demons techniques are considered to be very accurate methods to address NRR medical imaging. However, in the process to find very complex deformations, these approaches (OF and Demons) may find displacement fields that could lead to physically impossible deformations or foldings in the structures of interest, since these methods do not limit in this sense, the resulting transformations. Then, the Demons-based algorithm was updated to limit the search to diffeomorphic transformations by Vercauteren et al., proposing the Diffeomorphic Demons registration (DiffDem) [10].

2.1 Local Uncertainty Quantification

As mentioned in the introduction, FLR methods are limited to register images with matched intensities. Therefore, for the case of multimodal images or images with intensity variations, we propose to apply an initial mapping to the studied images (I_S, I_T) in order to overcome the intensity dependence by using a measure that describes the intensity uncertainty around each voxel [15]. This mapping has to transform both images into a common domain, where each voxel in one image could be compared with its counterpart in the other one, despite their mismatched intensities.

Suppose that a voxel $\mathbf{r} \in \Omega$ in an scene is described by the intensity uncertainty around it, and not by its own intensity value, then the following mapping could be defined:

$$I(\mathbf{r}) = F\left(I^m(\mathbf{r}), n\right), \tag{4}$$

where m indicates the image modality (MRI, CT, etc.), and n is the neighbourhood radius centred at each voxel $\mathbf{r}$. To define the local uncertainty quantification mapping (LUQ) $F(\cdot,\cdot)$, only metrics that do not depend on the intensity level of the voxels, but on their intensity uncertainty around its neighbours elements should be used, and a measure that meets this description is the entropy by quantifying it inside a neighbourhood of the voxel of interest. Thus, the LUQ is defined as follows,

$$F\left(I^m(\mathbf{r}), n\right) = -\sum_{\mathbf{u}\in \mathrm{W}_{\mathbf{r}}^n} p_{\mathbf{r}}\left(I^m(\mathbf{u})\right) \cdot \log\left[p_{\mathbf{r}}\left(I^m(\mathbf{u})\right)\right], \tag{5}$$

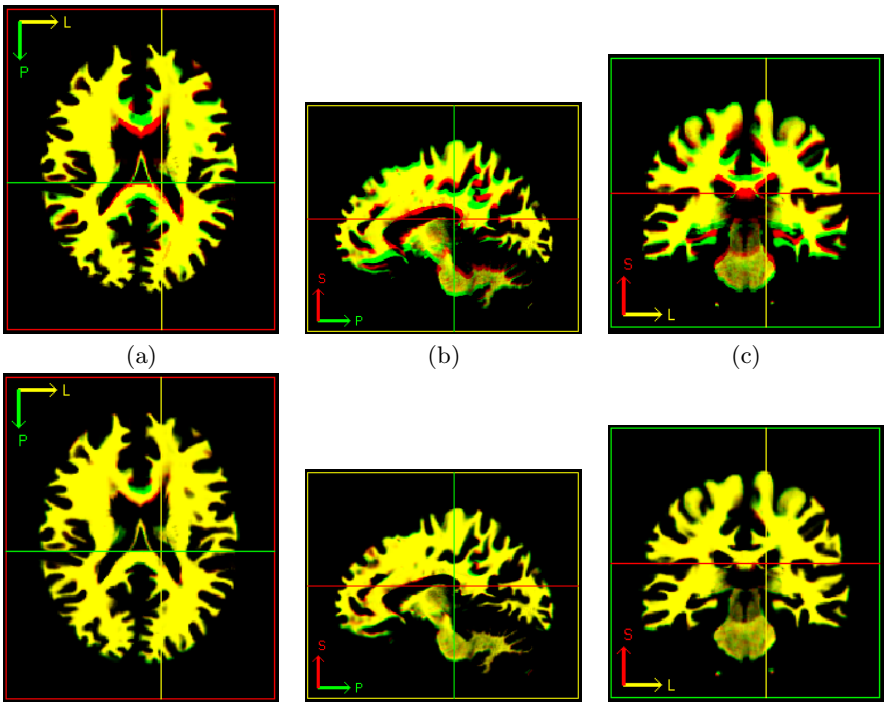

Fig. 2. Example of (a) Transversal, (b) sagittal and (c) coronal planes of white-matter matter overlapping in RGB colormap (in the green channel the target volume and in the red channel the source volume) before registration. (d) Transversal, (e) sagittal and (f) coronal plane of white-matter overlapping in RGB colormap (in the green channel the target volume and in the red channel the source volume), after registration with DiffDem+LUQ method. The yellow color indicates the overlapped zones.

where $\mathrm{W}_{\mathbf{r}}^{n}$ represents the set of voxels centred at $\mathbf{r}$ and with radius n, i.e.

$$\mathrm{W}_{\mathbf{r}}^{n} = \{\hat{\mathbf{r}} \in \Omega \mid \|\hat{\mathbf{r}} - \mathbf{r}\| \leq n\}, \tag{6}$$

and $p_{\mathbf{r}}(\cdot)$ is the local probability distribution of the image intensities within $\mathrm{W}_{\mathbf{r}}^{n}$. In this way, if the same object is appearing in two images (taken from the same scene), and if images do not distort or modify the shape of the observed element, the evaluation of LUQ in eq. (5) will be the same, regardless the intensities that describe the object into the image. Namely, eq. (1) can be satisfied for $I_T^{m_1}$ and $I_S^{m_2}$ with $m_1 \neq m_2$, (different images sequences or modalities), if these analyzed images are mapped through eq. (5).

2.2 Proposed Algorithm

Given a source image $I_S^{m_2}$ to be registered with a target one $I_T^{m_1}$ with intensities mismatched between them ($m_1 \neq m_2$), and a radius n to quantify the local

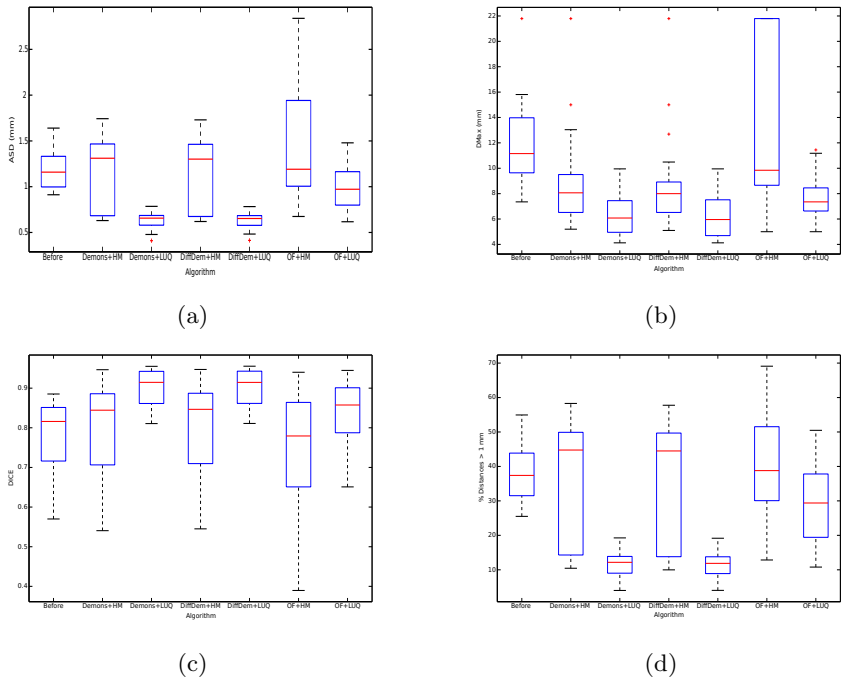

Fig. 3. Box plots of (a) ASD, (b) DMax, (c) DICE and (d) % of Distances > 1 mm for the 36 analyzed structures, before registration and after registration with Demons, DiffDem and OF with HM and LUQ transformations.

uncertainty, the proposed methodology for multimodal NRR can be seen as a flowchart in Fig. 1 and described as follows:

1. Obtain the images I_T and I_S from $I_T^{m_1}$ and $I_S^{m_2}$, through of LUQ according to equation (5): $I_T(\mathbf{r}) = F\left(I_T^{m_1}(\mathbf{r}), n\right)$ and $I_S(\mathbf{r}) = F\left(I_S^{m_2}(\mathbf{r}), n\right)$.
2. Apply an histogram matching [16] between I_T and I_S, in order to standardize their scales.
3. Find the non-parametric transformation Φ (displacements vector field $d(\cdot)$) between I_T and I_S using one of the FLR techniques (OF, Demons or DiffDem) [10, 13].
4. Apply the non-parametric transformation Φ to $I_S^{m_2}$, to finally deduce the elastic registered image as $I_R^{m_2} = I_S^{m_2} \circ \Phi$, such that the spatial correspondence between $I_T^{m_1}$ and $I_R^{m_2}$ is optimal.

It is important to note that the registration accuracy will depend on the selection of the radius n, whose optimal value may vary according to the type of the studied images, noise and voxel position $\mathbf{r}$ into the images (i.e. representing tissues, bone, etc.). The problem to estimate the optimal value of n according to the characteristics of the images will be addressed in future work, but in

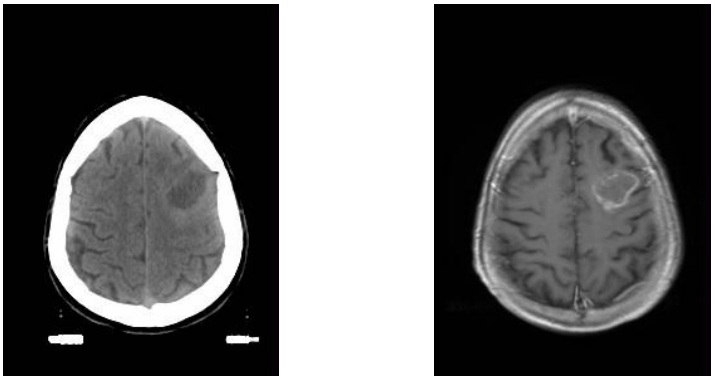

(a) (b)

Fig. 4. (a) Transversal slice of the CT image before medical treatment. (b) Transversal slice of the MRI after medical treatment.

Table 1. DICE, ASD, DMax and % of Distances > 0.8 mm for the cancerous tumour before CT-MRI registration, and after CT-MRI registration using Demons, DiffDem and OF with HM and LUQ transformations

Indice	**Algorithm**						
	Before	*Dem+HM*	*Dem+LUQ*	*DiffDem+HM*	*DiffDem+LUQ*	*OF+HM*	*OF+LUQ*
DICE	0.817	0.656	0.861	0.694	0.858	0.210	0.789
ASD (mm)	1.274	2.957	1.116	2.692	1.143	6.447	1.850
DMAx (mm)	8.526	9.945	8.526	9.234	8.526	48.773	9.000
% Distances > 0.8 mm	43.373	78.659	35.709	77.058	36.734	91.687	59.820

this paper, the radius was established empirically by a trial-and-error method with a value of $n = 2$. The FLR methods used in this work were implemented by using the libraries provided by the Insight Segmentation and Registration Toolkit (ITK) for medical image processing.

3 Experiments and Results

In order to evaluate the performance of the proposed registration strategy into a controlled scenario, multiparametric 3D MRIs (T1, T2 and PD weighted images) from a simulated brain database provided by Brain Web [17] were used. Multiparametric MRIs provide a proper dataset to test the addition of the LUQ step to FLR methods due to the presence of anatomic correspondence with mismatched intensities. The analyzed 3D images have a voxel size of $1.0 \times 1.0 \times 1.0$ mm. Four controlled elastic deformations were generated by applying transformation vector fields obtained from thin-plate splines, and these mappings were used as Ground Truths (gt), leading to a total of 12 sets of images to be registered ($T1_{gt}$-T2, $T1_{gt}$-PD and $T2_{gt}$-PD).

Then, a comparison between three FLR methods with LUQ (OF+LUQ, Demons+LUQ and DiffDem+LUQ), and three FLR strategies with an histogram

matching (OF+HM, Demons+HM and DiffDem+HM) were carried out. To evaluate the performance of each registration strategy, three segmented structures of the brain were employed (brain-spinal fluid, white-matter and gray-matter) to compute standard indices usually adopted for registration accuracy assessment: the DICE similarity coefficient, the average symmetric distance (ASD), the maximum symmetric distance (DMax), and the % of distances greater than the voxel dimension (1 mm) [18]. These indices were calculated before and after the registration process, given a total of 36 anatomical structures evaluated for each performance index. An example of the registration results for the white-matter structure by using the DiffDem+LUQ approach is shown in Fig. 2. Here we can observe the overlapping structures in RGB colormap in the transversal, sagittal and coronal planes, before and after the registration, where it is evident the recovery of the misalignment, especially in the inner zones of the brain.

Figure 3 shows the box-plots of the performance indices studied in this work for the 36 analyzed structures. In all four indices (DICE, ASD, DMax and % of distances greater than 1 mm), the Demons-based approaches with the LUQ initial transformation (Dem+LUQ and DiffDem+LUQ) had the best performance for this experiment. It is important to mention that the best results were achieved by the DiffDem approach. For the DICE index, DiffDem+LUQ presented a median value above 0.90, in comparison with a median of 0.82 before registration. For DMax, ASD and % of distances greater than 1 mm, the median values obtained with DiffDem+LUQ were 6.2 mm, 0.6 mm and 11.6% respectively, compared to 12.1 mm, 1.2 mm and 37.9% before registration. In addition, Fig. 3 shows that the addition of only a histogram matching step to the FLR methods for a registration process with multiparametric MRIs is not a viable option, since some performances indices did not improve after the registration, such as Demons+HM and DiffDem+HM for the ASD and % of distances greater than 1 mm indices, and OF+HM in DICE and % of distances greater than 1 mm.

We also carried out a second experiment to evaluate the proposed methodology with real clinical data, where a CT volume (see Fig. 4.(a)) was registered with a 3D MR image (see Fig. 4.(b)) of the brain. Both volumetric images were taken from a patient before (CT image) and after (MRI) undergoing a radiotherapy treatment for brain tumour. In this case, the clinical purpose is to recover the tumour deformation after radiotherapy, in order to obtain more information about the evolution of the medical treatment, which according of our proposed registration method this task could be possible because we expect to have same anatomic counterparts (the tumour) in the images to register. The tumour was segmented by an expert observer, and then DICE, ASD, DMax and % of distances greater than 0.8 mm (since for the volumes used in this experiment the resolution is $0.89 \times 0.89 \times 3.0$ mm for voxel) were computed before and after registration by using the same algorithms described in the previous experiment (Demons, DiffDem and OF with LUQ or HM). Our results are shown in Table 1, where the best performance was obtained again by DiffDem+LUQ with DICE, ASD and % of distances greater than 0.8 mm with values of 0.86, 1.14 mm and

36.73% respectively, compared to 0.82, 1.27 mm and 43.37% before the registration process. It is important to note that the tumour is a small structure, and for this reason is expected to achieve a lower improvement in the indices. Moreover, the results obtained for this clinical case show again that the addition of the HM step to FLR methods is not enough to achieve an accurate registration of multimodal images, as we expected.

4 Conclusions and Future Work

In this work, we proposed the use of local intensity uncertainty quantification in order to overcome the intensity conservation constraint of FLR algorithms. This novel fully automatic registration strategy was evaluated by using both synthetic (3D multiparametric MR brain images), and real (CT-MR brain images from a clinical case) deformations. Our results show that the addition of LUQ to the FLR methods improved considerably the performance of the NRR process in comparison to the common histogram matching step in multiparametric images, being the Diffeomorphic Demons approach with LUQ the best methodology. Our findings suggest that the proposed approach could be considered as a good option for the NRR of images with mismatched intensities but with the constraint of having the same anatomic counterparts in both images. In addition, the results suggest that the DiffDem+LUQ algorithm could work properly for multimodal cases. As future work, the proposed approach will be compared against the state of the art multimodal 3D registration algorithms to further validate its use in medical imaging.

References

1. Zitová, B., Flusser, J.: Image registration methods: a survey. Image and Vision Computing 21, 977–1000 (2003)
2. Modersitzki, J.: Numerical Methods for Image Registration. Oxford University Press (2004)
3. Crum, W., Hartkens, T., Hill, D.: Non-rigid image registration: theory and practice. British Journal of Radiology 77(spec. iss. 2), S140 – S153 (2004)
4. Mani, V., Rivazhagan, D.: Survey of medical image registration. Journal of Biomedical Engineering and Technology 1(2), 8–25 (2013)
5. Rueckert, D., Aljabar, P.: Nonrigid registration of medical images: Theory, methods, and applications. IEEE Signal Processing Magazine 27(4), 113–119 (2010)
6. Vásquez-Osorio, E.M., Hoogeman, M.S., Bondar, L., Levendag, P.C., Heijmen, B.J.M.: A novel flexible framework with automatic feature correspondence optimization for nonrigid registration in radiotherapy. Medical Physics 36(7), 2848–2859 (2009)
7. Pluim, J.P.W., Maintz, J., Viergever, M.: Mutual-information-based registration of medical images: a survey. IEEE Transactions on Medical Imaging 22(8), 986–1004 (2003)
8. Zhuang, X., Arridge, S., Hawkes, D., Ourselin, S.: A nonrigid registration framework using spatially encoded mutual information and free-form deformations. IEEE Transactions on Medical Imaging 30(10), 1819–1828 (2011)

9. Hui, W., Yong, Y., Hongjun, W., Guanzhong, G.: A modified optical flow based method for registration of 4d ct data of hepatocellular carcinoma patients. In: 2012 IEEE International Conference on Virtual Environments Human-Computer Interfaces and Measurement Systems (VECIMS), pp. 21–25 (2012)
10. Vercauteren, T., Pennec, X., Perchant, A., Ayache, N.: Diffeomorphic demons: Efficient non-parametric image registration. NeuroImage 45(1, suppl. 1), S61 – S72 (2009)
11. Janssens, G., Jacques, L., de Xivry, J.O., Geets, X., Macq, B.: Diffeomorphic registration of images with variable contrast enhancement. International Journal of Biomedical Imaging 2011, 3:1–3:12 (2011)
12. Baker, S., Scharstein, D., Lewis, J., Roth, S., Black, M., Szeliski, R.: A database and evaluation methodology for optical flow. International Journal of Computer Vision 92(1), 1–31 (2011)
13. Arce-Santana, E., Campos-Delgado, D.U., Alba, A.: A non-rigid multimodal image registration method based on particle filter and optical flow. In: Bebis, G., et al. (eds.) ISVC 2010, Part I. LNCS, vol. 6453, pp. 35–44. Springer, Heidelberg (2010)
14. Thirion, J.P.: Image matching as a diffusion process: an analogy with maxwell's. Medical Image Analysis 2, 243–260 (1988)
15. Reducindo, I., Mejia-Rodriguez, A.R., Arce-Santana, E.R., Campos-Delgado, D.U., Vigueras-Gomez, F., Scalco, E., Bianchi, A.M., Cattaneo, G.M., Rizzo, G.: Multimodal non-rigid registration methods based on local variability measures in computed tomography and magnetic resonance brain images. IET Image Processing (2014)
16. Nyul, L., Udupa, J., Zhang, X.: New variants of a method of mri scale standardization. IEEE Transactions on Medical Imaging 19(2), 143–150 (2000)
17. Kwan, R., Evans, A., Pike, G.: Mri simulation-based evaluation of image-processing and classification methods. IEEE Transactions on Medical Imaging 18(11), 1085–1097 (1999)
18. Heimann, T., Van Ginneken, B., Styner, M., Arzhaeva, Y., Aurich, V., Bauer, C., et al.: Comparison and evaluation of methods for liver segmentation from ct datasets. IEEE Transactions on Medical Imaging 28(8), 1251–1265 (2009)